Analysis of Inter-Bundle Crosstalk in Multimode Signaling for High-Density Interconnects

Yongjin Choi[1], Henning Braunisch[2], Kemal Aygün[2], and Paul D. Franzon[1]
[1]Department of Electrical and Computer Engineering, North Carolina State University, Raleigh, NC 27606
[2]Intel Corporation, Chandler, AZ 85226
E-mail: {ychoi, paulf}@ncsu.edu, {henning.braunisch, kemal.aygun}@intel.com

Abstract

While the increasing demand for smaller packages and low-cost platforms aggressively drives the interconnect density per unit area, crosstalk noise due to capacitive and inductive coupling limits the achievable interconnect density. As an alternative, we investigate multimode signaling where *n* signals are transmitted by exciting all fundamental modes on a group of *n* closely coupled lines called a bundle. Even though crosstalk is ideally zero in a single bundle, practical implementation of this idea for a typical input/output (IO) bus requires multiple closely-placed bundles. Thus, inter-bundle crosstalk may be an issue. In this paper, we analyze the inter-bundle crosstalk starting with the analytical expressions for the modal conversion from one bundle to another. Frequency domain simulations for both frequency-dependent and frequency-independent terminations are performed to compare performance vs. density benefits of multi-bundle multi-mode interconnects to those provided by conventional single-ended and differential signaling.

Introduction

The industry demand for smaller packages and low-cost platforms in conjunction with an aggressive scaling of the input/output (I/O) bandwidth of multicore microprocessors requires interconnects of maximized density per unit area. However, the increase of interconnect density can be achieved mainly by properly controlling crosstalk noise electrically or geometrically. The effort to reduce crosstalk in conventional signaling schemes such as single-ended or differential signaling includes electrical cancel-out, channel coding, and adaptive equalizers where crosstalk noise is considered as random noise and independent from the given interconnect. The attempt to reduce the number of interconnects includes line sharing [1]. To simultaneously achieve multi-gigabit per second (Gb/s) speed and high interconnect density, we consider an alternative signaling scheme that exploits multiple lines as a unit interconnect based on the well-known multiconductor transmission line theory [2], [3]. We call this alternative scheme for dense interconnects *multimode signaling* where *n* parallel signals are transmitted as the linear combination of *n* fundamental modes through a group of *n* tightly coupled lines called a *bundle* as illustrated in Fig. 1. The basic idea here is not new. Collaborate data transmission through multiple lines has been suggested by Nguyen and Scott [4]. Later Broyde and Clavelier [5] elaborated on their results by emphasizing the importance of a matched termination network connecting wire-to-wire. In this paper, recognizing that in practice a wide interconnect bus must be divided into bundles each associated with individual bundle transceivers and terminations we consider the interaction between such bundles. Numerical examples are given for realistic package level interconnect structures.

In multimode signaling, by exploiting the *n* modes extracted from the bundle-specific RLGC per-unit-length parameters (matrices of resistances, inductances, conductances, and capacitances) in given *n* lines along with a ground reference, we can effectively reduce the crosstalk at the receiving end. In Fig. 1 the encoder realizes the linear combination of *n* modes of the corresponding bundle and the decoder performs an inverse operation of the encoder. A matched termination network defined in [5] has been connected to suppress the reflection at the receiving end. $\mathbf{d} = [d_1, d_2, \ldots, d_n]$ represents *n* parallel source signals before encoding and $\mathbf{d'} = [d'_1, d'_2, \ldots, d'_n]$ the decoded ones, resulting in ideally $\mathbf{d} = \mathbf{d'}$.

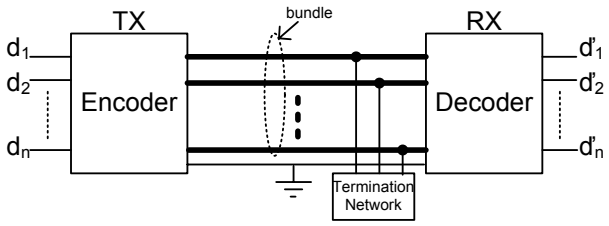

Figure 1. Multimode signaling on a single bundle.

To achieve high interconnect density with multimode signaling, it is required to analyze inter-bundle crosstalk when multiple closely-placed bundles are deployed. Knowledge of the inter-bundle crosstalk as a function of bundle-to-bundle spacing will give us an indication of the achievable interconnect density with multiple bundles. In differential signaling, a rule of thumb of differential pair spacing for avoiding severe crosstalk noise is about 4 or 5 times the dielectric height. The comparison of the density of multimode signaling to the one of differential signaling will be given in the later section with an example interconnect structure.

Inter-Bundle Crosstalk

In this section, we show how to account for inter-bundle crosstalk in terms of the coupled modal currents when multimode signaling is being employed. This is analogous to the mixed-mode S-parameters describing the mode conversion between differential and common modes in conventional differential signaling. The majority of the analysis is to formulate a two-bundle problem with ABCD parameters and boundary conditions. A simple scheme of examining the effect of bundle spacing on inter-bundle crosstalk is also presented.

Consider two identical bundles (comprising of microstrips or strip lines, for example) placed parallel to each other,

where a bundle consists of n uniform coupled conductor lines and a reference ground (Fig. 2). The two bundles are separated by the bundle-to-bundle spacing bs. Here we assume that an aggressor is bundle 1 and bundle 2 consists of quiet lines. The vector source $\mathbf{I}_S = [I_{S1}, I_{S2},\ldots, I_{Sn}]^t$ is connected to the left end (the near end) of bundle 1 where $[.]^t$ is the transpose of [.]. All ends of the bundles are terminated with an admittance (impedance) equal to the characteristic admittance (impedance) $\mathbf{Y}_{Cn}$ ($\mathbf{Z}_{Cn}$) of a single bundle in isolation, obtained in the limit of $bs \to \infty$. Under the quasi-TEM assumption, the electrical behavior of the two-bundle system is governed by the telegrapher's equation in phasor form [2],

$$-\frac{d\mathbf{V}(z)}{dz} = \mathbf{Z}\,\mathbf{I}(z), \quad -\frac{d\mathbf{I}(z)}{dz} = \mathbf{Y}\,\mathbf{V}(z) \tag{1}$$

where $\mathbf{V} = [V_1^{(1)},..., V_n^{(1)}, V_1^{(2)},..., V_n^{(2)}]^t$ is the $2n \times 1$ column vector of line voltages and $\mathbf{I} = [I_1^{(1)},..., I_n^{(1)}, I_1^{(2)},..., I_n^{(2)}]^t$ the $2n \times 1$ column vector of line currents on the two bundles at position z along the bundles. Here $V_j^{(i)}$ and $I_j^{(i)}$ are the j-th line voltage and current, respectively, on bundle i. Furthermore, $\mathbf{Z} = \mathbf{R} + j\omega\mathbf{L}$ is the $2n \times 2n$ per-unit-length (p.u.l.) impedance matrix and $\mathbf{Y} = \mathbf{G} + j\omega\mathbf{C}$ is the $2n \times 2n$ p.u.l. admittance matrix. $\mathbf{R}$, $\mathbf{L}$, $\mathbf{G}$, and $\mathbf{C}$ are $2n \times 2n$ p.u.l. resistance, inductance, conductance, and capacitance matrices, respectively.

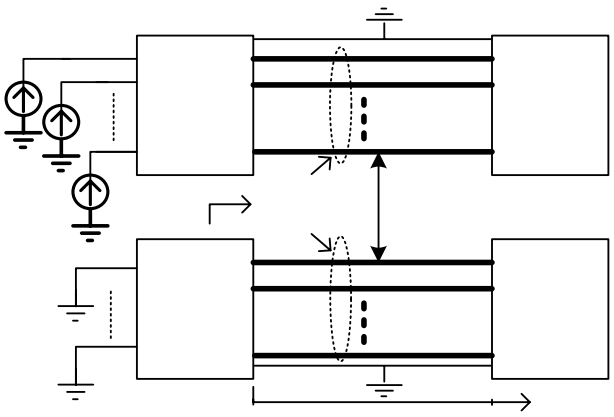

Figure 2. Inter-bundle crosstalk between two bundles.

Since generally n conductors have n propagation modes, line voltages and currents can be expressed as a superposition of modal voltages $\mathbf{V}_m$ and currents $\mathbf{I}_m$ by using transformation matrices $\mathbf{T}_V$ and $\mathbf{T}_I$, respectively. Each column of the $2n \times 2n$ $\mathbf{T}_V$ (or $\mathbf{T}_I$) matrix consists of the eigenvectors of $\mathbf{ZY}$ (or $\mathbf{YZ}$). As a first step, to describe the line voltages and currents of the two bundles at both ends ($z = d$, $z = 0$) of the lines, ABCD parameters (or chain parameters) each of size $2n \times 2n$ can be employed in matrix form:

$$\begin{bmatrix}\mathbf{V}(d)\\ \mathbf{I}(d)\end{bmatrix} = \begin{bmatrix}\mathbf{A}(d) & \mathbf{B}(d)\\ \mathbf{C}(d) & \mathbf{D}(d)\end{bmatrix}\begin{bmatrix}\mathbf{V}(0)\\ \mathbf{I}(0)\end{bmatrix} \tag{2}$$

Here the ABCD parameters for the system of two bundles of length d are defined as [2]

$$\mathbf{A}(d) = \mathbf{Z}_C \cosh(\sqrt{\mathbf{YZ}}d)\mathbf{Y}_C \qquad \mathbf{B}(d) = -\mathbf{Z}_C \sinh(\sqrt{\mathbf{YZ}}d)$$
$$\mathbf{C}(d) = -\sinh(\sqrt{\mathbf{YZ}}d)\mathbf{Y}_C \qquad \mathbf{D}(d) = \cosh(\sqrt{\mathbf{YZ}}d) \tag{3}$$

where $\mathbf{Y}_C$ ($\mathbf{Z}_C$) is the characteristic admittance (impedance) of the two coupled bundles obtained by $\mathbf{Z}^{-1}\mathbf{T}_V\mathbf{\Gamma}\mathbf{T}_V^{-1}$ [6]. Note that here $\mathbf{\Gamma}$ is a $2n \times 2n$ diagonal matrix whose elements are the eigenvalues of $\mathbf{YZ}$. To derive the input impedance $\mathbf{Z}_{in}$, we need to rewrite (2) as

$$\begin{bmatrix}\mathbf{V}(0)\\ \mathbf{I}(0)\end{bmatrix} = \begin{bmatrix}\mathbf{A}(d) & -\mathbf{B}(d)\\ -\mathbf{C}(d) & \mathbf{D}(d)\end{bmatrix}\begin{bmatrix}\mathbf{V}(d)\\ \mathbf{I}(d)\end{bmatrix} \tag{4}$$

With $\mathbf{V}(d) = \mathbf{Z}_L\mathbf{I}(d)$ and $\mathbf{V}(0) = \mathbf{Z}_{in}\mathbf{I}(0)$, we can obtain $\mathbf{Z}_{in}$ as

$$\mathbf{Z}_{in} = [\mathbf{A}(d)\mathbf{Z}_L - \mathbf{B}(d)][\mathbf{D}(d) - \mathbf{C}(d)\mathbf{Z}_L]^{-1} \tag{5}$$

where $\mathbf{Z}_L = [\,\mathbf{Z}_{Cn}\ \mathbf{0}_n;\ \mathbf{0}_n\ \mathbf{Z}_{Cn}\,]$ with $\mathbf{0}_n$ the $n \times n$ zero matrix. From the boundary condition

$$\mathbf{I}(0) = \mathbf{I}_S' - \mathbf{Z}_L^{-1}\mathbf{Z}_{in}\mathbf{I}(0)$$

$\mathbf{I}(0)$ and $\mathbf{V}(0)$ can be expressed as

$$\mathbf{I}(0) = (\mathbf{U}_{2n} + \mathbf{Z}_L^{-1}\mathbf{Z}_{in})^{-1}\mathbf{I}_S' \tag{6}$$

$$\mathbf{V}(0) = \mathbf{Z}_{in}\mathbf{I}(0) \tag{7}$$

where $\mathbf{I}_S' = [\mathbf{I}_S, 0,...,0]^t$ is a $2n \times 1$ column vector and $\mathbf{U}_{2n}$ the $2n \times 2n$ unity matrix. Therefore, $\mathbf{I}(d)$ and $\mathbf{V}(d)$ can be obtained from $\mathbf{I}_S$ and the ABCD parameters based on (2).

One approach to measure inter-bundle crosstalk for multimode signaling is to examine the modal conversion between bundles. Since multimode signaling transmits a linear combination of n modes, inter-bundle crosstalk can be considered as equivalent to measuring the coupled mode signals on bundle 2, $\mathbf{I}_m^{j(2)}$, by exciting each mode at bundle 1, $\mathbf{I}_m^{j(1)}$, where j denotes the j-th mode of a bundle ($j = 1,\ldots, n$). From (2), (6), and (7), we can obtain the line current $\mathbf{I}^{(2)}(d)$ with $\mathbf{I}_S = \mathbf{I}_m^{j(1)}$ and thereby the coupled mode current $\mathbf{I}_m^{j(2)}$ as

$$\mathbf{I}_m^{j(2)}(d) = \mathbf{T}_{In}^{-1}\mathbf{I}^{(2)}(d) \tag{8}$$

where $\mathbf{T}_{In}$ is an $n \times n$ matrix in which each column is an eigenvector of $\mathbf{Y}_n\mathbf{Z}_n$. Here $\mathbf{Y}_n$ ($\mathbf{Z}_n$) is the $n \times n$ p.u.l. admittance (impedance) matrix of a single bundle ($bs \to \infty$). If we extract $2n \times 2n$ matrices of $\mathbf{Z}$ and $\mathbf{Y}$ with varying bundle spacing (bs) and obtain the coupled mode current at bundle 2, $\mathbf{I}_m^{j(2)}$ from (8), the inter-bundle crosstalk can be quantified as a function of bs. In the next section, the inter-bundle crosstalk of an example interconnect is presented with varying bundle spacing when exciting each mode at bundle 1.

Numerical Example

For demonstrating the inter-bundle crosstalk analysis in the previous section numerically, we consider an embedded microstrip bundle consisting of four lines as shown in Fig. 3. The line width, spacing, and thickness are 20 μm, 20 μm, and 15 μm, respectively. The thickness of solder mask, substrate, and reference plane are 20 μm, 25 μm, and 15 μm, respectively.

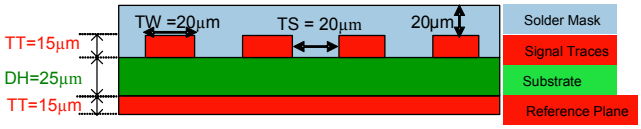

Figure 3. Example of a bundle on a package substrate (cross-section).

The bundle RLGC matrices of the example can be obtained from a 2-D electromagnetic field solver such as Ansoft 2D Extractor as illustrated in Fig. 4. From the small values of **R** [Fig. 4(a)] and **G** [Fig. 4(c)] we can justify the low-loss assumption of quasi-TEM analysis. The coupling values of capacitance [Fig. 4(d)] and inductance [Fig. 4(b)] are $C_m / C_{ii} = 0.33$ and $L_m / L_{ii} \approx 0.25$, respectively. Note that capacitance values in the example are frequency-independent because of all conductors having high conductivity and dielectric constants are assumed to be frequency-independent; correspondingly, **G** in Fig. 4(c) exhibits the expected linear behavior (frequency-independent loss tangents). The frequency dependency of **R** and **L** is related to the skin effect for conductors of finite conductivity. The four modes of the example bundle are illustrated in Fig. 5 with a propagation constant, $\gamma = \alpha + j\beta$ of each mode, where α is the attenuation constant and β is the phase constant. Each mode can be characterized by the attenuation constants because the differences of phase constants of four modes are very small.

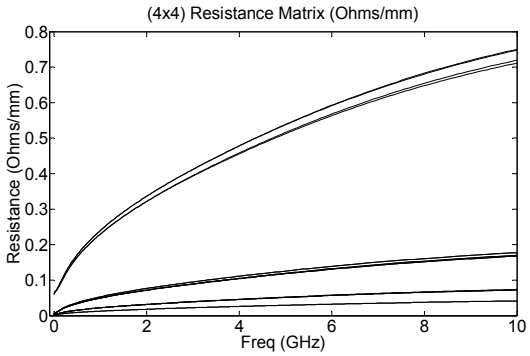

(a) Resistance per-unit-length **R**.

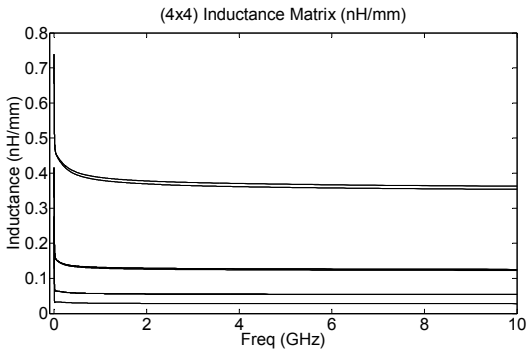

(b) Inductance per-unit-length **L**.

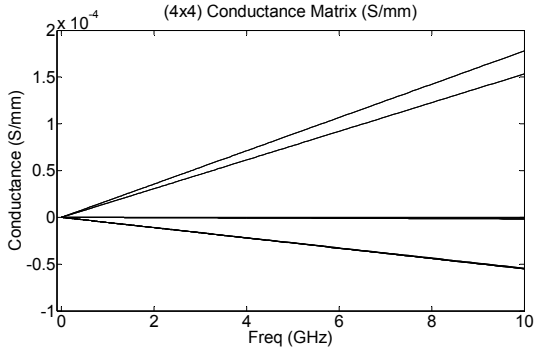

(c) Conductance per-unit-length **G**.

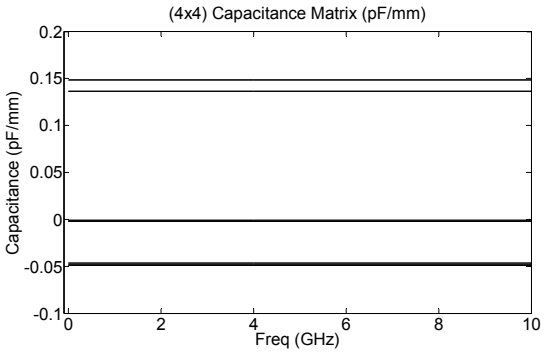

(d) Capacitance per-unit-length **C**.

Figure 4. Per-unit-length matrices **R**, **L**, **G**, and **C** of size 4 x 4.

Two example bundles are configured as an interconnect of embedded microstrip lines consisting of eight parallel lines. The line length is set to 2 cm, a nominal diagonal length on typical flip chip ball/land grid array (FCBGA/FCLGA) packages. The simulation setup follows the configuration of Fig. 2: Both ends of the bundles are terminated with the characteristic admittance $\mathbf{Y}_{C4}$ of an individual bundle (obtained in absence of the other bundle). The left end of bundle 1 is excited with a current mode eigenvector $\mathbf{I}_S = \mathbf{I}_m^{j(1)}$, a column vector of $\mathbf{T}_{I4}$ (4×4 matrix) among four modes in the frequency domain. By using ABCD parameters and the boundary conditions, the line currents of bundle 2 at $z = 2$ cm are calculated, that is, the crosstalk noise coupled to bundle 2 with respect to a modal current $\mathbf{I}_m^{j(1)}$. To examine the potential density benefit of multimode signaling, we need to simulate the coupled mode currents with different RLGC matrices corresponding to the varying bundle spacing. Here we consider two cases of bundle spacings: $bs = 100$ μm for the weakly coupled case and $bs = 20$ μm for the case of strongly coupled bundles. To explore the possibility of the practical application of multimode signaling, the responses with non-matched termination such as passive elements directly connected between ends of lines and reference ground have also been computed.

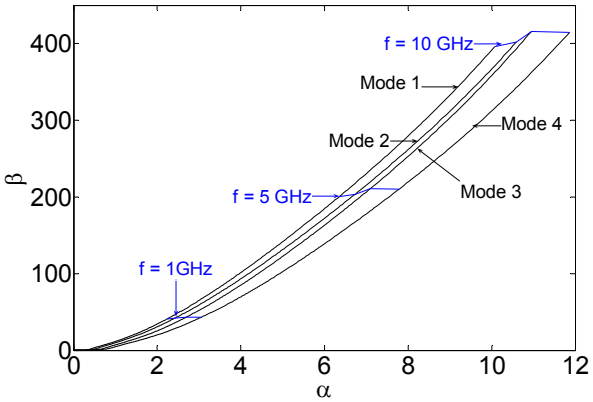

Figure 5. Four modes of the example bundle represented by propagation constant, $\gamma = \alpha + j\beta$ of each mode, where α is the attenuation constant and β the phase constant. The blue lines indicate α and β of each mode corresponding to the same frequency.

A. With frequency-dependent termination $\mathbf{Y}_{L4}(f)$

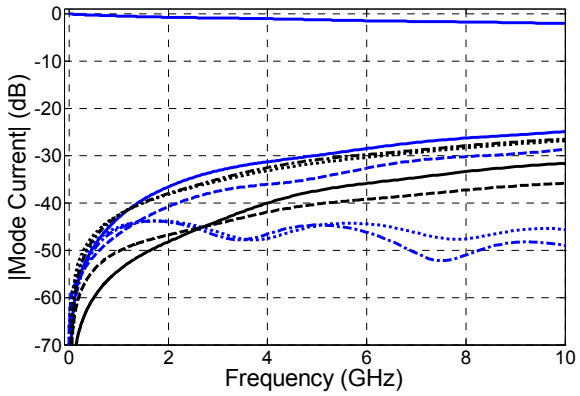

Figure 6. The far-end coupled mode currents at bundle 2 due to excitation of mode 1 currents at bundle 1 with frequency-dependent matched termination for bundle spacing of 20 μm (blue) and 100 μm (black).

All ends of the bundles are terminated with the characteristic admittance $\mathbf{Y}_{L4}(f)$ of the example bundle derived for each frequency. Fig. 6 demonstrates the mode conversion coupled to the adjacent bundle 2 by exciting the mode 1 currents at bundle 1 for two different values of bundle spacing (*bs* = 20 μm and 100 μm). This is done by plotting the coupled modal currents on bundle 2, $\mathbf{I}_m^{j(2)}(d = 2\text{ cm})$, when bundle 1 is excited with mode 1, 2, 3, or 4. As a representative example the mode 1 current vector, $\mathbf{I}_S = \mathbf{I}_m^{1(1)}$, is excited. The far-end response on bundle 1 is shown by the top line of Fig. 6 (insertion loss). The black lines are the coupled modal currents on bundle 2 when *bs* = 100 μm and the blue lines (except the line at the top) are the coupled modal currents on bundle 2 when *bs* = 20 μm for the four current modes. Considering the plots for all four modes, we can see that only a few dB increase result by reducing the bundle spacing from 100 μm to 20 μm. This implies that the inter-bundle crosstalk noise increases less than two times in magnitude when the bundle spacing is reduced by five times. Crosstalk magnitude is < –25 dB up to 10 GHz.

B. With frequency-independent termination ($\mathbf{Y}_{L4}$ = const.)

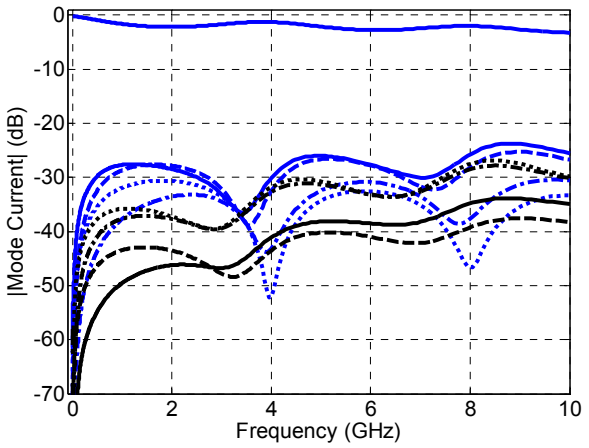

Figure 7. The far-end coupled mode currents at bundle 2 due to excitation of mode 1 currents at bundle 1 with frequency-independent termination for bundle spacing of 20 μm (blue) and 100 μm (black).

In practice, it would be difficult to make a termination network $\mathbf{Y}_{L4}$ having a specified wide-range frequency-dependent response using passive elements. Therefore, as a second numerical experiment, $\mathbf{Y}_{L4}$ is set to be a diagonal matrix in which each diagonal element is 1/50 S, thereby anticipating reflections due to an imperfectly matched termination. Fig. 7 illustrates the far-end coupled mode currents on bundle 2 by connecting the admittance of 1/50 S between the ends of the lines and reference ground. All other conditions are the same as for Fig. 6. We observe resonances at certain frequencies indicating imperfect termination. Depending on the bundle spacing, the far-end coupled mode currents have shifted up by up to about 10 dB. Compared with the matched termination (Fig. 6) reflections from the imperfect termination affect lower frequencies more severely than those above 6 GHz. Cross-talk magnitude in this example remains < –23 dB up to 10 GHz.

C. With frequency-independent termination and a fixed source current mode 1

In general, the modal currents, the column vectors of $\mathbf{T}_{I4}$ functioning as a source current at bundle 1, are frequency-dependent unless the cross-section of the interconnect structure is cyclic symmetric [2]. But the practical application calls for a frequency-independent $\mathbf{T}_{I4}$ working as an encoder in multimode signaling (Fig. 1). In Fig. 8, the source mode 1 current $\mathbf{I}_S = \mathbf{I}_m^{1(1)}$ is set to the value when the arbitrarily selected frequency is 5 GHz. Compared to case B above, the fixed $\mathbf{T}_{I4}$ does not affect the coupled noise, as the magnitude variation of mode currents with respect to frequencies is very small in this example.

D. With frequency-independent termination and exciting four modes summed together

Since the multimode signaling utilizes the linear combination of all the bundle modes, we now consider a source current $\mathbf{I}_S$ that is the sum of all the four current modes. Note that each current mode is taken as frequency-independent. All other conditions are the same as case C. The

results are shown in Fig. 9. We can notice that crosstalk magnitude still remains < -23 dB up to 10 GHz by reducing the bundle spacing up to 20 µm.

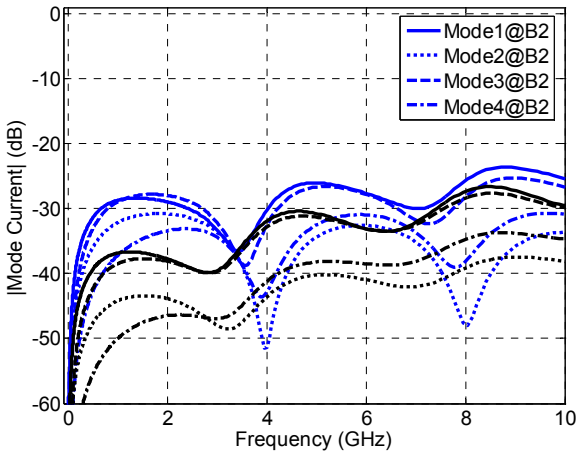

Figure 8. The far-end coupled mode currents at bundle 2 due to excitation of the frequency-independent mode 1 current at bundle 1 with the frequency-independent termination for bundle space 20 µm (blue) and 100 µm (black).

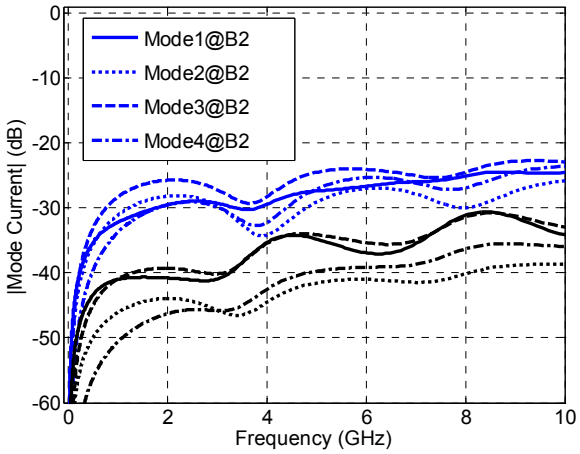

Figure 9. The far-end coupled mode currents on bundle 2 due to excitation of the frequency-independent four mode currents summed together at bundle 1 with frequency-independent termination and for bundle spacing 20 µm (blue) and 100 µm (black).

The near-end inter-bundle crosstalk for two bundle spacing (20 µm and 100 µm) also presents the similar results, that is, the near-end inter-bundle crosstalk < -20dB for all four cases (A, B, C, and D). To see the density benefit of multimode interconnects compared to the conventional differential signaling, the far-end differential crosstalk (DFEXT) is illustrated in Fig. 10 for two values of differential pair spacing (20 µm and 100 µm). The DFEXT increases over three times in magnitude when reducing the differential pair spacing by five times. This implies that the density benefit of multimode signaling is ideally two times to the differential signaling because the differential signaling consumes two lines per signal transmission and the far-end crosstalk noise is about the same for both signaling.

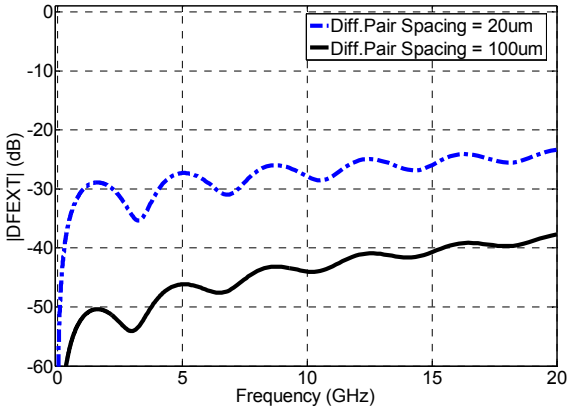

Figure 10. The far-end differential crosstalk for differential pair spacing 20 µm (blue) and 100 µm (black).

Conclusions

The analysis and simulation of inter-bundle crosstalk for high-density multimode signaling has been developed based on multiconductor transmission line theory. Intra-bundle (as opposed to inter-bundle) crosstalk can be investigated similarly. The reduction of bundle spacing in conjunction with a couple of different conditions (frequency-dependent / independent terminations and frequency-independent codec) has kept the inter-bundle crosstalk magnitude less than -20 dB. The comparison of the far-end crosstalk noise with the one of conventional differential signaling indicates that higher density per the effective signal transmission becomes feasible with multimode signaling, provided that all other conditions are the same for both signaling. Time-domain simulation combined with a non-linear transceiver model will provide more reliable results with the estimation of the multimode system performance.

Acknowledgments

This research was supported by the Semiconductor Research Corporation through Intel custom funding.

References

1. A. Carusone, K. Farzan, and D. A. Johns, "Differential signaling with a reduced number of signal paths," *IEEE Trans. Circuits Syst. II*, vol. 48, no. 3, pp. 294–300, Mar. 2001.
2. C. R. Paul, *Analysis of Multiconductor Transmission Lines*. Wiley-Interscience, 1994.
3. J. B. Faria, *Multiconductor Transmission-Line Structures*. Wiley, 1993.
4. T. H. Nguyen and T. R. Scott, "Propagation over multiple parallel transmission lines via modes," *IBM Technical Disclosure Bulletin*, vol. 32, no. 11, pp. 1–6, April 1990.
5. F. Broyde and E. Clavelier, "A new method for the reduction of crosstalk and echo in multiconductor interconnections," *IEEE Trans. Circuits Syst. I*, vol. 52, no. 2, pp. 405–416, Feb. 2005.
6. C. R. Paul, "Decoupling the multiconductor transmisssion line equations," *IEEE Trans. Microwave Theory Tech.*, vol. 44, no. 8, pp. 1429–1440, Aug. 1996.